

Dynamical mean-field study of Vanadium diselenide monolayer ferromagnetism

Taek Jung Kim¹, Siheon Ryee¹, Myung Joon Han^{1*} and Sangkook Choi^{2*}

¹Department of Physics, KAIST, 291 Daehak-ro, Yuseong-gu, Daejeon 34141, Republic of Korea

²Condensed Matter Physics and Materials Science Department, Brookhaven National Laboratory, Upton, NY 11973, USA

E-mail: mj.han@kaist.ac.kr, sachoi@bnl.gov

November 2019

Abstract. To understand the magnetism of VSe₂, whose monolayer form has recently been reported to be a room temperature ferromagnet, Here, the combined method of conventional density functional theory with dynamical mean-field theory has been adopted. This higher-level computation method enables us to resolve many of existing controversies and contradictions in between theory and experiment. First of all, this new approach is shown to give the correct magnetic properties of both bulk and two-dimensional limit of VSe₂ which demonstrates its superiority to the conventional methods. The results demonstrate that monolayer VSe₂ without charge density waves is a ferromagnet with ordering temperature of 250K. From the direct simulation of temperature-dependent magnetic susceptibility and ordered moment, it is shown that its ferromagnetism is clearly two-dimensional in nature. Further, it is shown that this ferromagnetic order is vulnerable to extra charge dopings which provides the important insight to elucidate recent experimental controversies.

1. Introduction

Two-dimensional (2D) magnetism has played central roles in numerous scientific and technological advancements including high temperature superconductivity, quantum Hall related phenomena, and the development of new devices.[1–17] In the past couple of years, notable magnetic orders have been observed even in single atomic layers. [18–22] These 2D magnetic van der Waals materials are expected to open up a wide range of possibilities. The vast phase space with different elements and structures suggests the straightforward tuning of its magnetic properties. Moreover, due to the ease of fabricating 2D heterostructures, magnetic van der Waals materials have a great potential to provide a new unit for multifunctional devices. [23–26]

Among them, one of the fascinating materials is 1T-VSe₂. [21, 27–34] This layered compound is composed of the ABC-stacked Se-V-Se atomic sheets (Figure 1(a)). Since each V atom is surrounded by six Se, ionically V-*d* states are split into *t*_{2g} and *e*_g manifolds. Due to the trigonal distortion, *t*_{2g} degeneracy is further lifted to form higher-lying *a*_{1g} and two-fold degenerate *e*_g^{π±} states as depicted in Figure 1(a). Most interestingly, VSe₂ monolayer is claimed to be a 2D ferromagnet with Curie temperature (*T*_c) above room temperature. [21, 33, 35] It is particularly interesting because bulk VSe₂ remains paramagnetic down to low temperature. [27, 28, 30, 36]

However, this conclusion remains elusive both theoretically and experimentally. For example, the reported experimental moments of $\approx 15\mu_B$ [21] or $5\mu_B$ [33] are too large to be compared with the calculated values of about $0.6\mu_B$. [37–39] While a more recent experiment reports a much reduced moment of $\approx 0.31\mu_B$ [35], the inconsistency needs to be further studied. Furthermore, other experimental studies report the absence of ferromagnetic order for the same material, [32, 34] which certainly requires a thorough theoretical investigation. The claim of monolayer ferromagnetism heavily relies on the first-principles calculation result based on DFT-GGA (density functional theory within generalized gradient approximation) which consistently produces the ferromagnetic ground state. [37, 38] An obvious problem is, however, that DFT-GGA predicts the ferromagnetic phase also for the bulk VSe₂ being in a sharp contrast to the experimental fact of paramagnetism. [27, 28, 30, 36, 38, 40]

In order to perform a reliable investigation, one needs the higher-level theoretical framework suited for both itinerant and localized characters of electrons associated with the open-*d* shells. First-principles methods in combination with dynamical mean-field theory (DMFT) provide an efficient way to study the dual nature of electrons by mapping a quantum many-body lattice problem onto a multi-orbital quantum impurity problem in an effective electron bath. [41] We hereby adopt the charge self-consistent LDA+DMFT to investigate the magnetic properties of VSe₂. For the construction of DMFT computations, the on-site Coulomb interaction parameters (Hubbard *U* and Hund *J*_H) associated with V-*d* orbitals have been calculated within constrained random phase approximation (cRPA) [42–44], and the nominal double-counting scheme [45] is used for the self-energy correction (see Figure 1(b, c) and Computational methodology section for more details).

2. Computational methods

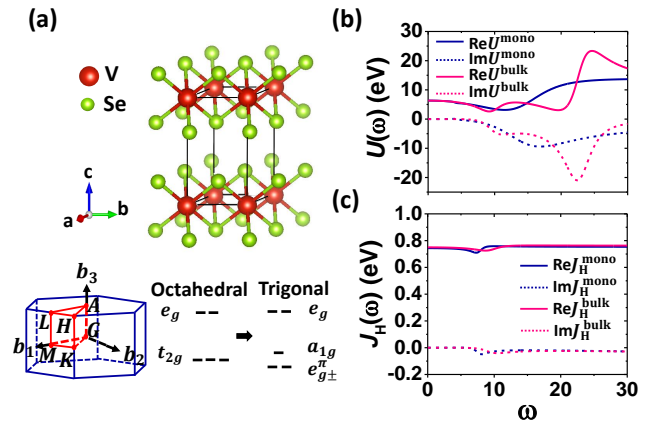


Figure 1. (a) Crystal structure of bulk 1T-VSe₂, high symmetry points in the first Brillouin zone, and schematic picture for the crystal field level splitting. Red and green spheres represent vanadium and selenium atom respectively. Due to the trigonally distorted octahedron, *t*_{2g} states split into *a*_{1g} and *e*_g^{π±}. (b, c) The ω -dependent Coulomb (b) and Hund (c) interaction parameter calculated by cRPA for both monolayer (blue) and bulk (magenta) VSe₂. Solid and dashed lines present the real and imaginary parts, respectively.

The calculations have been performed by all-electrons DFT code Wien2K [46], EDMFTF [47], and ComDMFT package[48]. GGA functional

parameterized by Perdew, Burke, and Ernzerhof [49] was adopted. The k-point grids of $16 \times 16 \times 7$ and $26 \times 26 \times 1$ were used for bulk and monolayer VSe₂, respectively. Crystal structure was determined by internal relaxation within GGA functional with the fixed experimental cell parameters [27, 28, 34, 50–52] and the force criterion of 0.5 mRyd per Å. For monolayer calculation, the vacuum layer of 30 Å has been taken into account. For on-site Coulomb interaction parameters, we used the cRPA technique [42–44] as implemented in ComDMFT package. [48] For the calculation of the partially screened Coulomb interaction, we chose the transitions between the bands in the hybridization energy window from -10 to $+4$ eV, and defined the polarizability from the transitions as our low-energy polarizability.

Figure 1(b, c) show the ω -dependent Hubbard U and Hund J_H as obtained from our cRPA. As well known, J_H is almost ω -independent [53, 54]. While $U(\omega)$ exhibits the more ω dependence, its behavior becomes nearly flat in the small ω regime which supports the conventional way of using static $U(\omega = 0)$ value. Considering all these facts and following most of literature, we adopted the static value of U and J_H in the current study. We also checked the U and J_H dependence of our conclusion by varying $\pm 20\%$ of these interaction parameters from cRPA values. It is found that none of our conclusion is changed. The main change is the slight enhancement of moment formation when the larger values are used as expected. The change of (monolayer) moment at 100K is about $0.03\mu_B$ and $0.25\mu_B$ for the U and J_H change, respectively. It is also noted that the effect of ω -dependence can effectively be understood by the use of slightly greater static U value [55, 56].

The nominal double counting scheme has been adopted with 3 electron occupation in the V-d orbitals as predicted by DFT-GGA. ‡ § In order to properly describe the trigonally distorted local environment around V-d orbitals, we adopted a local basis set that diagonalizes the matrix $\epsilon_{imp} + \text{Re}\Delta(\omega = 0)$ (where, ϵ_{imp} : impurity levels, $\Delta(\omega)$: hybridization function between local impurity and bath) during LDA+DMFT charge self-consistent calculation. Our LDA+DMFT calculations were performed by using Wien2K+EDMFTF. We also double-checked the result of paramagnetic phases using ComDMFT built on top of FlapwMBPT code [57] for *ab initio* LDA

‡ See also the experimental report by Cao *et al.* which shows that the valance electron number in VSe₂ is closer to the vanadium metal (d^3) rather than that of VO₂ (d^1)

§ We have also repeated calculations with another widely-used double counting choice, namely, ‘fully localized limit (FLL)’ functional. While the use of FLL seems to slightly enhance ferromagnetism by producing a slightly larger monolayer moment of $0.438\mu_B$ at 100K, no other noticeable change has been found.

calculations.

3. Results and discussion

Figure 2(a, b) show the calculated electronic structure of monolayer and bulk VSe₂, respectively, in comparison with the previous angle-resolved photoemission spectroscopy (ARPES) data by Feng *et al.* [34]. Red, blue and green colors represent the result of LDA+DMFT in their paramagnetic phases, non-magnetic GGA, and ARPES spectra in the paramagnetic temperature regime, [34] respectively. Two different theories coincidentally predict that both monolayer and bulk 1T-VSe₂ are metals and that the interlayer coupling in bulk is not negligible; see, for example, the dispersive bands along G-A and K-H lines (Figure 2(b)).

It should be noted that the dynamical local correlation (which is missing in LDA or GGA calculation) plays an essential role for the description of important details around the Fermi level. Figure 2(a, b) clearly show that LDA+DMFT results are in better agreement with experiments. See, for example, the G-M line in the range of -0.5 - 0.0 eV; the ARPES result (green crosses) of the highest valence band significantly deviates from the GGA band structure (blue dashed lines), exhibiting the larger (smaller) effective mass (band velocity). We also found that the calculation result of modified Becke-Johnson (MBJ) functional [58, 59] is similar with that of LDA/GGA. These notable features related to the electronic correlation are well-captured by DMFT (the red colored). The renormalized bands are mainly of V- $e_{g\pm}^{\pi}$ and V- a_{1g} orbital character as demonstrated by projected density of states (PDOS) in Figure 2(c, e). The effect of correlation can be quantified by the quasiparticle weight defined as $Z = (1 - \frac{\partial \text{Im}\Sigma_{ii}(i\omega_n)}{\partial \omega_n}|_{\omega_n = \frac{\pi}{\beta}})^{-1}$ where Σ_{ii} is the electronic self-energy associated with the orbital i and β is the inverse temperature; The band velocity and effective mass is renormalized by factor of Z and $1/Z$, respectively. Figure 2(d, f) show the calculated Z factors for each V- d orbital in 1T-VSe₂ monolayer and bulk, respectively. It is clearly shown that the correlation strengths in both systems are strongly orbital dependent. The Z factors for two V- e_g orbitals (blue triangles) are about 0.7 and basically temperature independent. In contrast, Z for V- $e_{g\pm}^{\pi}$ (green squares) and V- a_{1g} (red circles) are significantly smaller, ~ 0.4 , and decrease upon cooling in both bulk and monolayer.

To resolve the key issue in this material, namely, the possible monolayer ferromagnetism, we calculated the ferromagnetic order parameter $m = \mu_B(\langle n_{\uparrow} \rangle - \langle n_{\downarrow} \rangle)$ (where μ_B is Bohr magneton and $\langle n_{\uparrow(\downarrow)} \rangle$ is the up(down)-spin electron occupation in the V- d subshell)

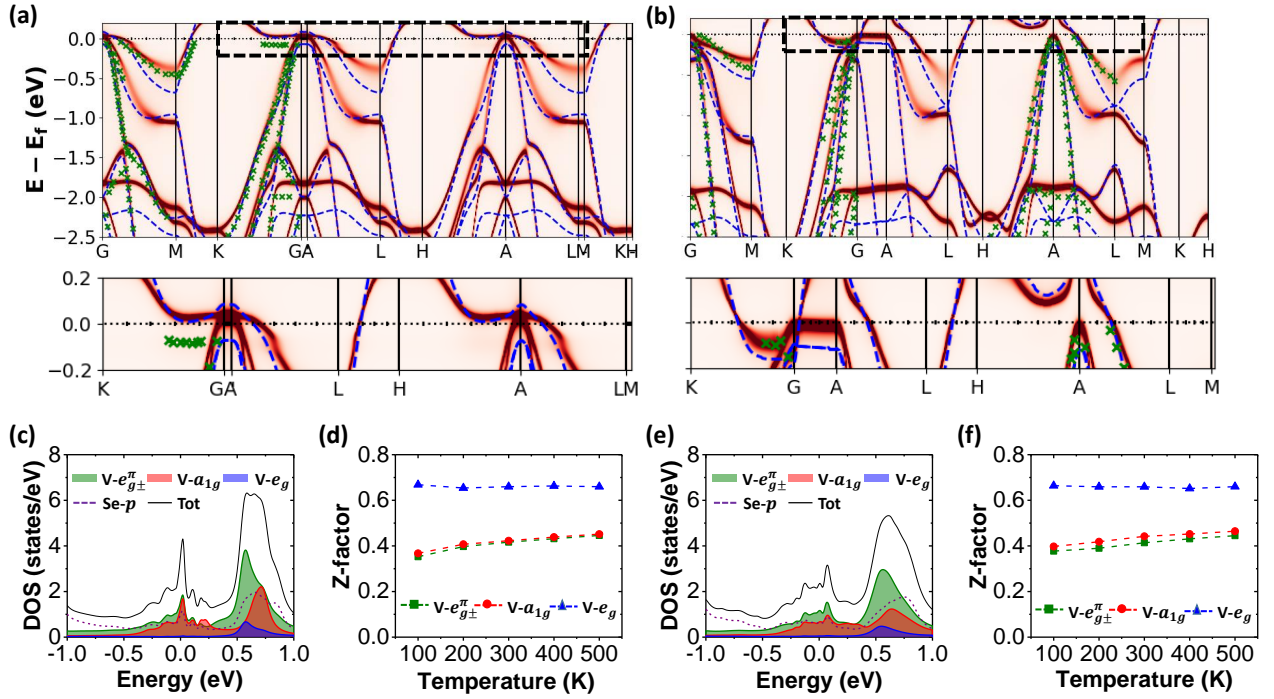


Figure 2. The calculated electronic structure and the quasiparticle weight Z . (a, b) LDA+DMFT band dispersion of monolayer (a) and bulk (b) VSe₂, respectively, in comparison with GGA and ARPES data. Red, blue and green colors represent the results of charge self-consistent LDA+DMFT spectral functions (at 300K), non-magnetic GGA, and ARPES [34]. The black dashed box regions in the upper panels are enlarged in the lower panels. (c, e) The calculated PDOS of monolayer (c) and bulk (e) VSe₂ within charge-self-consistent LDA+DMFT. In the case of the monolayer, a well defined van Hove singularity peak appears at Fermi level whereas it is broadened in bulk. Green, red, blue colors represent e_g^π , a , and e_g orbital states, respectively. The dashed and solids black lines show the $Se-p$ and total DOS, respectively. (d, f) The calculated quasiparticle weight associated with $V-d$ orbitals in the monolayer (d) and bulk (f) 1T-VSe₂.

as a function of temperature; see Figure 3(a). The magenta squares and the blue triangles represent the LDA+DMFT results for monolayer and bulk VSe₂, respectively. The first thing to be noted is the absence of ferromagnetic order for the bulk phase as known from experiments. Note that GGA predicts the ferromagnetic order even for bulk, which significantly undermines its predictability for the magnetic ground state of monolayer VSe₂. [37, 38, 40]

For monolayer, our LDA+DMFT calculation clearly shows that ferromagnetic order is developed and the magnetic moment is about $0.37\mu_B$. In this regard, our result is seemingly in better agreement with the previous experimental reports of monolayer ferromagnetism [21, 33, 35] rather than paramagnetism. [32, 34] Also, it is in good agreement with a recent XMCD (x-ray magnetic circular dichroism) measurement [35] rather than the older experimental reports [21, 33]. As for the critical temperature, however, the calculated $T_c \approx 250K$ is markedly lower than the experimental value of $T_c \geq 300K$ [21, 33, 35] These differences might reflect the presence of charge density wave (CDW) phase whose temperature range varies from 120K to 360K

depending on experiments. [21, 33, 34, 52] There can be certain types of extrinsic effects in experimental situations such as defects and/or the interaction with substrate. Or, the difference of about 50K can be reconciled simply by taking slightly greater U or/and J_H value than cRPA ones. Considering the discrepancy even among the experimental T_c and the various unexplored possibilities, any quantitative comparison needs to be careful. In the below we pursue the deeper understanding of magnetism in VSe₂.

Figure 3(b) presents the temperature dependent local spin susceptibility $\chi_m = \int_0^\beta d\tau \langle m(\tau)m(0) \rangle$ (where τ is an imaginary time) which clearly shows the localized moments formed in the monolayer. Magenta squares and blue circles are the result of monolayer (χ_m^{mono}) and bulk (χ_m^{bulk}) susceptibility, respectively. For the latter, Pauli-like temperature-independent behavior demonstrates the electron delocalization in bulk VSe₂, being consistent with experimental report. [36] For the former, on the other hands, χ_m^{mono} exhibits the weak but clear inverse-temperature dependence, indicative of the electron localization (see the inset). This local nature is another important new aspect that LDA+DMFT reveals for VSe₂ magnetism. We also

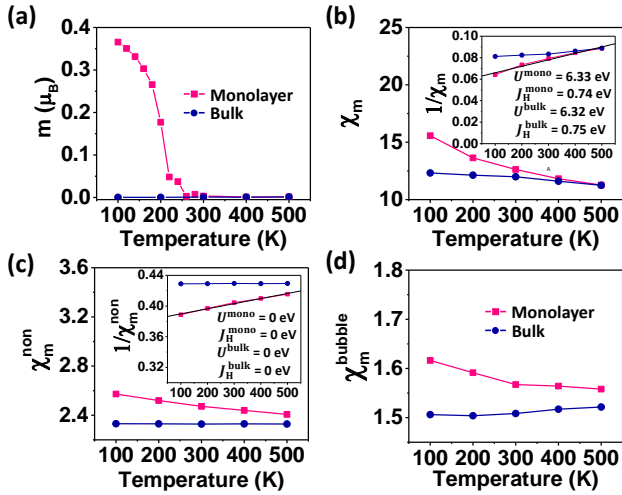


Figure 3. (a) The calculated ferromagnetic order parameter $m = \mu_B(\langle n_\uparrow \rangle - \langle n_\downarrow \rangle)$ as a function of temperature. The magenta line with squares and the blue with circles present the result for monolayer and bulk VSe₂, respectively. For monolayer, ferromagnetic transition is clearly identified at around 250K. (b) The calculated local spin susceptibility $\chi_m = \int_0^\beta d\tau \langle m(\tau)m(0) \rangle$ as a function of temperature. The inset shows the inverse susceptibilities which clearly show Curie- and Pauli-like behavior for monolayer and bulk, respectively. (c) The calculated non-interacting local spin susceptibility ($U = J_H = 0$) of bulk (blue circles) and monolayer (magenta squares) in their paramagnetic phases. The inset presents its inverse. (d) The spin susceptibility calculated within bubble approximation.

found that the localized moment is formed mainly in the $V-e_{g\pm}^\pi$ and $V-a_{1g}$ orbitals.

In the following paragraphs, we argue that this local behavior in the monolayer VSe₂ is attributed to the concerted effect of reduced dimensionality and electronic correlation. Figure 3(c) shows the calculated non-interacting spin susceptibilities (χ_m^{non} ; $U=J_H=0$) in monolayer (magenta squares) and bulk (blue circles) in their paramagnetic phases. Note that the bulk susceptibility ($\chi_{m,\text{bulk}}^{\text{non}}$) exhibits the Pauli-like behavior whereas the inverse-temperature dependence is clearly identified for the monolayer susceptibility ($\chi_{m,\text{mono}}^{\text{non}}$; see the inset). Note that this behavior of $\chi_{m,\text{mono}}^{\text{non}}$ is solely attributed to the band structure (without interaction effect), particularly to the van Hove singularity near the Fermi level. [60–64] As shown in Figure 2(a), van Hove singularity is strongly enhanced in the monolayer VSe₂, implying the vanishing electron velocity; compare the dispersions along K-G and H-A line in Figure 2(a) to 2(b). This electronic behavior naturally leads to the saddle-point formation \parallel and the divergence in DOS. For the

\parallel The van Hove singularity of monolayer VSe₂ is in the G-K and A-H line along which the near-Fermi-level band makes a minimum while it does a maximum along the orthogonal direction to those lines, forming a saddle point

bulk, on the other hand, the inter-layer coupling is noticeable; for example, compare the dispersion along the M-K-G path to that along H-A-L (Figure 2(a, b)). It naturally weakens the van Hove singularity leading to the broader DOS near the Fermi energy as shown in Figure 2(c, e). This characteristic band feature of monolayer VSe₂ is the effect of reduced dimensionality.

The local dynamical correlation plays a crucial role on top of the pre-localization of electrons caused by two dimensionality. We found that the correlation enhances the electron localization in two distinctive ways. First, the local dynamical correlation renormalizes the electronic structure, especially the bands with the critical point. The orbital character of these bands are mainly $V-e_{g\pm}^\pi$ and $V-a_{1g}$ as shown in Figure 2(d, f). Their Z^{-1} values greater than two demonstrate the strong enhancement of electron localization caused by the band structure renormalization. It can further be confirmed by comparing χ_m^{non} to the spin susceptibility within bubble approximation; $\chi_m^{\text{bubble}} = 2\mu_B^2 \sum_{i,j \in V-d} \int_0^\beta d\tau G_{i,j}(\tau) G_{j,i}(-\tau)$ (where $G_{i,j}$ is a LDA-DMFT local Green’s function). As shown in Figure 3(c, d), χ_m^{non} is almost two times greater than χ_m^{bubble} . It is consistent with the Z^{-1} value of $V-e_{g\pm}^\pi$ and $V-a_{1g}$ orbitals, demonstrating that this enhancement originates from the band renormalization. Second, in addition to the quasiparticle band structure effect, the dynamical correlation facilitates the electron localization in the two-particle level. Compared to χ_m^{bubble} , the spin susceptibility, χ_m , is strongly enhanced; compare the magenta line in Figure 3(b) with that in Figure 3(d). Its temperature dependence is also more pronounced than χ_m^{bubble} , indicative of the important contribution coming from vertex correction to the spin susceptibility of vanadium.

Here we stress that the reduced dimensionality is essential for the local moment formation as demonstrated by the fact that the bulk susceptibility, $\chi_{m,\text{bulk}}$, remains temperature-independent; see Figure 3(b). Namely, the electronic correlation alone cannot induce the moment formation even if the $\chi_{m,\text{bulk}}$ is significantly greater $\chi_{m,\text{bulk}}^{\text{non}}$ in the entire temperature range. As the origin of local moment formation, the combined effect of dimensional reduction and electron correlation is not just physically interesting but also possibly important to understand experiments. For example, it implies that the local moment can be suppressed by the inter-layer hoppings or the monolayer-substrate interactions.

In order to explore other possible reasons for the contradictory experimental reports on the monolayer ferromagnetism, [21, 32–35] one can consider both cation(or anion) defects and charge transfer from substrate as often observed in this type of chalcogenide systems.[30, 34, 65–73] In fact, our calculation shows

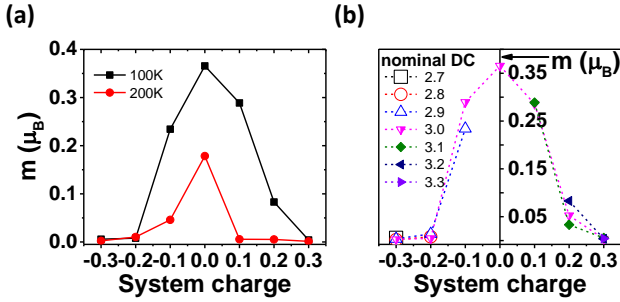


Figure 4. (a) The calculated ferromagnetic order parameter $m = \mu_B(\langle n_\uparrow \rangle - \langle n_\downarrow \rangle)$ for monolayer VSe₂ with a varying system charge at two different temperatures. The hole-like and electron-like extra charges have been introduced through the DFT system charge option (and the updated DMFT chemical potential accordingly). (b) The calculated m with a varying system charge together with nominal double-counting charge at T=100K. The seven different values for V-d occupations in the nominal double-counting choice have been considered ranging from -0.3 to $+0.3$ (the same with system charge range).

that the ferromagnetic order is vulnerable to the extra effective charges introduced. Figure 4 presents the calculated ferromagnetic moment m as a function of varying system charges. In Figure 4(a), we simulate the effect of both hole-like (negative values) and electron-like (positive values) extra charges by tuning the system charge at the DFT level while, in Figure 4(b), both DFT system charge and DMFT nominal double-counting value are simultaneously controlled. The results demonstrate that introducing the extra charges through, for example, V or Se defects, can easily suppress the ferromagnetic order. The number of extra charges (*i.e.*, $-0.3 \leq e \leq +0.3$) seems to be reasonable to simulate the possible defect concentrations considering the reported values of related systems such as Fe₃GeTe₂ and FeTe. [68, 70–73] This result hopefully provides useful information to understand the previous experimental reports and to stimulate the further investigations.

Finally, an important factor that has not been directly addressed in the current study is the cooperation or competition of ferromagnetism with CDW order. It is known that the monolayer VSe₂ also hosts the CDW order while the CDW vector can be different from its bulk counter part [21, 32–34, 52]. Importantly, all experiments that observed ferromagnetic signal coincidentally report the T_c well above T_{CDW} [21, 33, 35]. Thus, our result of ferromagnetic order in the undistorted 1T structure is quite meaningful. It is noted simultaneously that the formation of CDW phase likely suppresses the ferromagnetic order rather than enhances as noted in a recent study [39]. Considering many different reports on the temperature scale as well as the pattern of CDW [21, 33, 34, 52, 74], this issue certainly requires further

careful investigations in both theory and experiment.

4. Conclusion

We investigated the magnetic properties of bulk and monolayer VSe₂ by using charge self-consistent LDA+DMFT approach. Our results show that VSe₂ monolayer is a ferromagnetically-ordered material below 250K whereas its bulk phase is paramagnetic. The electron localization and subsequent local moment formation in the monolayer originate from the quasiparticle pre-localization enabled by the reduced dimensionality and its enhancement by local dynamical correlation. This study provides an important example where the reduced dimensionality is an essential factor to form local moments and subsequent magnetic orderings. Our work will be useful in the understanding and design of possible magnetic devices based on 2D heterostructures.

5. Acknowledgements

We thank J.-H. Sim and H.-S. Kim for useful technical discussion. T. J. Kim, S. Ryee and M. J. Han were supported by BK21plus program, Basic Science Research Program (2018R1A2B2005204) and Creative Materials Discovery Program through NRF (2018M3D1A1058754). T. J. Kim, S. Ryee and S. Choi were supported by the U.S Department of Energy, Office of Science, Basic Energy Sciences as a part of the Computational Materials Science Program. This research used resources of the National Energy Research Scientific Computing Center (NERSC), a U.S. Department of Energy Office of Science User Facility operated under Contract No. DE-AC02-05CH11231.

References

- [1] Lee P A, Nagaosa N and Wen X G 2006 *Reviews of Modern Physics* **78** 17–85 ISSN 0034-6861, 1539-0756 URL <https://link.aps.org/doi/10.1103/RevModPhys.78.17>
- [2] Fernandes R M, Chubukov A V and Schmalian J 2014 *Nature Physics* **10** 97–104 ISSN 1745-2473, 1745-2481 URL <http://www.nature.com/articles/nphys2877>
- [3] Scalapino D J 2012 *Reviews of Modern Physics* **84** 1383–1417 ISSN 0034-6861, 1539-0756 URL <https://link.aps.org/doi/10.1103/RevModPhys.84.1383>
- [4] Paglione J and Greene R L 2010 *Nature Physics* **6** 645–658 ISSN 1745-2473, 1745-2481 URL <http://www.nature.com/articles/nphys1759>

- [5] Nagaosa N, Sinova J, Onoda S, MacDonald A H and Ong N P 2010 *Reviews of Modern Physics* **82** 1539–1592 ISSN 0034-6861, 1539-0756 URL <https://link.aps.org/doi/10.1103/RevModPhys.82.1539>
- [6] Stormer H L, Laboratories B, Tsui D C and Gossard A C 1999 *Rev. Mod. Phys.* **71** 8
- [7] von Klitzing K 1986 *Reviews of Modern Physics* **58** 519–531 ISSN 0034-6861 URL <https://link.aps.org/doi/10.1103/RevModPhys.58.519>
- [8] Li J, Li Y, Du S, Wang Z, Gu B L, Zhang S C, He K, Duan W and Xu Y 2019 *Science Advances* **5** eaaw5685 ISSN 2375-2548 URL <http://advances.sciencemag.org/lookup/doi/10.1126/sciadv.aaw5685>
- [9] Liu Z, Zhao G, Liu B, Wang Z F, Yang J and Liu F 2018 *Physical Review Letters* **121** ISSN 0031-9007, 1079-7114 URL <https://link.aps.org/doi/10.1103/PhysRevLett.121.246401>
- [10] Cardoso C, Soriano D, García-Martínez N A and Fernández-Rossier J 2018 *Physical Review Letters* **121** ISSN 0031-9007, 1079-7114 URL <https://link.aps.org/doi/10.1103/PhysRevLett.121.067701>
- [11] Huang B, Clark G, Klein D R, MacNeill D, Navarro-Moratalla E, Seyler K L, Wilson N, McGuire M A, Cobden D H, Xiao D, Yao W, Jarillo-Herrero P and Xu X 2018 *Nature Nanotechnology* **13** 544–548 ISSN 1748-3387, 1748-3395 URL <http://www.nature.com/articles/s41565-018-0121-3>
- [12] Jiang S, Li L, Wang Z, Mak K F and Shan J 2018 *Nature Nanotechnology* **13** 549–553 ISSN 1748-3387, 1748-3395 URL <http://www.nature.com/articles/s41565-018-0135-x>
- [13] Jiang S, Shan J and Mak K F 2018 *Nature Materials* **17** 406–410 ISSN 1476-1122, 1476-4660 URL <http://www.nature.com/articles/s41563-018-0040-6>
- [14] Seyler K L, Zhong D, Klein D R, Gao S, Zhang X, Huang B, Navarro-Moratalla E, Yang L, Cobden D H, McGuire M A, Yao W, Xiao D, Jarillo-Herrero P and Xu X 2018 *Nature Physics* **14** 277–281 ISSN 1745-2473, 1745-2481 URL <http://www.nature.com/articles/s41567-017-0006-7>
- [15] Wang Z, Gutiérrez-Lezama I, Ubrig N, Kroner M, Gibertini M, Taniguchi T, Watanabe K, Imamoğlu A, Giannini E and Morpurgo A F 2018 *Nature Communications* **9** ISSN 2041-1723 URL <http://www.nature.com/articles/s41467-018-04953-8>
- [16] Wang Z, Zhang T, Ding M, Dong B, Li Y, Chen M, Li X, Huang J, Wang H, Zhao X, Li Y, Li D, Jia C, Sun L, Guo H, Ye Y, Sun D, Chen Y, Yang T, Zhang J, Ono S, Han Z and Zhang Z 2018 *Nature Nanotechnology* **13** 554–559 ISSN 1748-3387, 1748-3395 URL <http://www.nature.com/articles/s41565-018-0186-z>
- [17] Song T, Tu M W Y, Carnahan C, Cai X, Taniguchi T, Watanabe K, McGuire M A, Cobden D H, Xiao D, Yao W and Xu X 2019 *Nano Letters* **19** 915–920 ISSN 1530-6984, 1530-6992 URL <http://pubs.acs.org/doi/10.1021/acs.nanolett.8b04160>
- [18] Lee J U, Lee S, Ryoo J H, Kang S, Kim T Y, Kim P, Park C H, Park J G and Cheong H 2016 *Nano Letters* **16** 7433–7438 ISSN 1530-6984, 1530-6992 URL <http://pubs.acs.org/doi/10.1021/acs.nanolett.6b03052>
- [19] Huang B, Clark G, Navarro-Moratalla E, Klein D R, Cheng R, Seyler K L, Zhong D, Schmidgall E, McGuire M A, Cobden D H, Yao W, Xiao D, Jarillo-Herrero P and Xu X 2017 *Nature* **546** 270–273 ISSN 0028-0836, 1476-4687 URL <http://www.nature.com/articles/nature22391>
- [20] Fei Z, Huang B, Malinowski P, Wang W, Song T, Sanchez J, Yao W, Xiao D, Zhu X, May A F, Wu W, Cobden D H, Chu J H and Xu X 2018 *Nature Materials* **17** 778–782 ISSN 1476-1122, 1476-4660 URL <http://www.nature.com/articles/s41563-018-0149-7>
- [21] Bonilla M, Kolekar S, Ma Y, Diaz H C, Kalappattil V, Das R, Eggers T, Gutierrez H R, Phan M H and Batzill M 2018 *Nature Nanotechnology* **13** 289–293 ISSN 1748-3387, 1748-3395 URL <http://www.nature.com/articles/s41565-018-0063-9>
- [22] O'Hara D J, Zhu T, Trout A H, Ahmed A S, Luo Y K, Lee C H, Brenner M R, Rajan S, Gupta J A, McComb D W and Kawakami R K 2018 *Nano Letters* **18** 3125–3131 ISSN 1530-6984, 1530-6992 URL <http://pubs.acs.org/doi/10.1021/acs.nanolett.8b00683>
- [23] Zhong D, Seyler K L, Linpeng X, Cheng R, Sivadas N, Huang B, Schmidgall E, Taniguchi T, Watanabe K, McGuire M A, Yao W, Xiao D, Fu K M C and Xu X 2017 *Science Advances* **3** e1603113 ISSN 2375-2548 URL <http://advances.sciencemag.org/lookup/doi/10.1126/sciadv.1603113>
- [24] Kim H H, Yang B, Patel T, Sfigakis F, Li C, Tian S, Lei H and Tsen A W 2018 *Nano Letters* **18** 4885–4890 ISSN 1530-6984, 1530-6992 URL <http://pubs.acs.org/doi/10.1021/acs.nanolett.8b01552>

- [25] Song T, Cai X, Tu M W Y, Zhang X, Huang B, Wilson N P, Seyler K L, Zhu L, Taniguchi T, Watanabe K, McGuire M A, Cobden D H, Xiao D, Yao W and Xu X 2018 *Science* **360** 1214–1218 ISSN 0036-8075, 1095-9203 URL <http://www.sciencemag.org/lookup/doi/10.1126/science.aar4851>
- [26] Gong C and Zhang X 2019 *Science* **363** eaav4450 ISSN 0036-8075, 1095-9203 URL <http://www.sciencemag.org/lookup/doi/10.1126/science.aav4450>
- [27] Bayard M and Sienko M 1976 *Journal of Solid State Chemistry* **19** 325–329 ISSN 00224596 URL <https://linkinghub.elsevier.com/retrieve/pii/0022459676901845>
- [28] van Bruggen C and Haas C 1976 *Solid State Communications* **20** 251–254 ISSN 00381098 URL <https://linkinghub.elsevier.com/retrieve/pii/0038109876901873>
- [29] Strocov V N, Shi M, Kobayashi M, Monney C, Wang X, Krempasky J, Schmitt T, Patthey L, Berger H and Blaha P 2012 *Physical Review Letters* **109** ISSN 0031-9007, 1079-7114 URL <https://link.aps.org/doi/10.1103/PhysRevLett.109.086401>
- [30] Barua S, Hatnean M C, Lees M R and Balakrishnan G 2017 *Scientific Reports* **7** ISSN 2045-2322 URL <http://www.nature.com/articles/s41598-017-11247-4>
- [31] Pásztor A, Scarfato A, Barreateau C, Giannini E and Renner C 2017 *2D Materials* **4** 041005 ISSN 2053-1583 URL <http://stacks.iop.org/2053-1583/4/i=4/a=041005?key=crossref.dc634b45e8b82b836f1bc06b8eb3adc6>
- [32] Chen P, Pai W W, Chan Y H, Madhavan V, Chou M Y, Mo S K, Fedorov A V and Chiang T C 2018 *Physical Review Letters* **121** ISSN 0031-9007, 1079-7114 URL <https://link.aps.org/doi/10.1103/PhysRevLett.121.196402>
- [33] Duvjir G, Choi B K, Jang I, Ulstrup S, Kang S, Thi Ly T, Kim S, Choi Y H, Jozwiak C, Bostwick A, Rotenberg E, Park J G, Sankar R, Kim K S, Kim J and Chang Y J 2018 *Nano Letters* **18** 5432–5438 ISSN 1530-6984, 1530-6992 URL <http://pubs.acs.org/doi/10.1021/acs.nanolett.8b01764>
- [34] Feng J, Biswas D, Rajan A, Watson M D, Mazzola F, Clark O J, Underwood K, Marković I, McLaren M, Hunter A, Burn D M, Duffy L B, Barua S, Balakrishnan G, Bertran F, Le Fèvre P, Kim T K, van der Laan G, Hesjedal T, Wahl P and King P D C 2018 *Nano Letters* **18** 4493–4499 ISSN 1530-6984, 1530-6992 URL <http://pubs.acs.org/doi/10.1021/acs.nanolett.8b01649>
- [35] Yu W, Li J, Herng T S, Wang Z, Zhao X, Chi X, Fu W, Abdelwahab I, Zhou J, Dan J, Chen Z, Chen Z, Li Z, Lu J, Pennycook S J, Feng Y P, Ding J and Loh K P 2019 *Advanced Materials* **31** 1903779 ISSN 1521-4095 URL <https://onlinelibrary.wiley.com/doi/abs/10.1002/adma.201903779>
- [36] Cao Q, Yun F F, Sang L, Xiang F, Liu G and Wang X 2017 *Nanotechnology* **28** 475703 ISSN 0957-4484, 1361-6528 URL <http://stacks.iop.org/0957-4484/28/i=47/a=475703?key=crossref.d033a390ee2ed0033eba764acb4ecb6a>
- [37] Ma Y, Dai Y, Guo M, Niu C, Zhu Y and Huang B 2012 *ACS Nano* **6** 1695–1701 ISSN 1936-0851, 1936-086X URL <http://pubs.acs.org/doi/10.1021/nm204667z>
- [38] Li F, Tu K and Chen Z 2014 *The Journal of Physical Chemistry C* **118** 21264–21274 ISSN 1932-7447, 1932-7455 URL <http://pubs.acs.org/doi/10.1021/jp507093t>
- [39] Fumega A O and Pardo V 2018 *arXiv:1804.07102 [cond-mat]* (Preprint 1804.07102) URL <http://arxiv.org/abs/1804.07102>
- [40] Lebègue S, Björkman T, Klintonberg M, Nieminen R M and Eriksson O 2013 *Physical Review X* **3** ISSN 2160-3308 URL <https://link.aps.org/doi/10.1103/PhysRevX.3.031002>
- [41] Georges A, Kotliar G, Krauth W and Rozenberg M J 1996 *Reviews of Modern Physics* **68** 13–125 ISSN 0034-6861, 1539-0756 URL <https://link.aps.org/doi/10.1103/RevModPhys.68.13>
- [42] Aryasetiawan F, Imada M, Georges A, Kotliar G, Biermann S and Lichtenstein A I 2004 *Phys. Rev. B* **70** 195104 URL <http://link.aps.org/doi/10.1103/PhysRevB.70.195104>
- [43] Şaşıoğlu E, Friedrich C and Blügel S 2011 *Phys. Rev. B* **83** 121101 ISSN 1098-0121, 1550-235X URL <http://link.aps.org/doi/10.1103/PhysRevB.83.121101>
- [44] Choi S, Kutepov A, Haule K, van Schilfhaarde M and Kotliar G 2016 *Npj Quantum Materials* **1** 16001 URL <https://doi.org/10.1038/npjquantmats.2016.1>
- [45] Pourovskii L V, Amadon B, Biermann S and Georges A 2007 *Phys. Rev. B* **76**(23) 235101 URL <https://link.aps.org/doi/10.1103/PhysRevB.76.235101>
- [46] Blaha P, Schwarz K, Madsen G K H, Kvasnicka K and Luitz J 2001 *Technische Universität Wien, Austria*
- [47] Haule K, Yee C H and Kim K 2010 *Physical Review B* **81** ISSN 1098-0121, 1550-235X URL <https://link.aps.org/doi/10.1103/PhysRevB.81.195107>

- [48] Choi S, Semon P, Kang B, Kutepov A and Kotliar G 2018 *arXiv:1810.01679 [cond-mat]* (Preprint 1810.01679) URL <http://arxiv.org/abs/1810.01679>
- [49] Perdew J P, Burke K and Ernzerhof M 1996 *Phys. Rev. Lett.* **77** 3865–3868 URL <https://link.aps.org/doi/10.1103/PhysRevLett.77.3865>
- [50] Thompson A H and Silbernagel B G 1978 *Journal of Applied Physics* **49** 1477–1479 ISSN 0021-8979, 1089-7550 URL <http://aip.scitation.org/doi/10.1063/1.324929>
- [51] Liu Z L, Wu X, Shao Y, Qi J, Cao Y, Huang L, Liu C, Wang J O, Zheng Q, Zhu Z L, Ibrahim K, Wang Y L and Gao H J 2018 *Science Bulletin* **63** 419 – 425 ISSN 2095-9273 URL <http://www.sciencedirect.com/science/article/pii/S2095927318301233>
- [52] Umemoto Y, Sugawara K, Nakata Y, Takahashi T and Sato T 2019 *Nano Research* **12** 165–169 ISSN 1998-0124, 1998-0000 URL <http://link.springer.com/10.1007/s12274-018-2196-4>
- [53] Miyake T and Aryasetiawan F 2008 *Phys. Rev. B* **77**(8) 085122 URL <https://link.aps.org/doi/10.1103/PhysRevB.77.085122>
- [54] Vaugier L, Jiang H and Biermann S 2012 *Phys. Rev. B* **86**(16) 165105 URL <https://link.aps.org/doi/10.1103/PhysRevB.86.165105>
- [55] Werner P, Sakuma R, Nilsson F and Aryasetiawan F 2015 *Phys. Rev. B* **91**(12) 125142 URL <https://link.aps.org/doi/10.1103/PhysRevB.91.125142>
- [56] Casula M, Werner P, Vaugier L, Aryasetiawan F, Miyake T, Millis A J and Biermann S 2012 *Phys. Rev. Lett.* **109**(12) 126408 URL <https://link.aps.org/doi/10.1103/PhysRevLett.109.126408>
- [57] Kutepov A, Oudovenko V and Kotliar G 2017 *Computer Physics Communications* **219** 407–414 ISSN 0010-4655 URL <http://www.sciencedirect.com/science/article/pii/S0010465517301947>
- [58] Becke A D and Johnson E R 2006 *The Journal of Chemical Physics* **124** 221101 ISSN 0021-9606, 1089-7690 URL <http://aip.scitation.org/doi/10.1063/1.2213970>
- [59] Tran F and Blaha P 2009 *Phys. Rev. Lett.* **102** 226401 ISSN 0031-9007, 1079-7114 URL <https://link.aps.org/doi/10.1103/PhysRevLett.102.226401>
- [60] Mielke A and Tasaki H 1993 *Communications in Mathematical Physics* **158** 341–371 ISSN 0010-3616, 1432-0916 URL <http://link.springer.com/10.1007/BF02108079>
- [61] Ulmke M 1998 *The European Physical Journal B* **1** 301–304 ISSN 1434-6028 URL <http://link.springer.com/10.1007/s100510050186>
- [62] Wahle J, Blümer N, Schlipf J, Held K and Vollhardt D 1998 *Physical Review B* **58** 12749–12757 ISSN 0163-1829, 1095-3795 URL <https://link.aps.org/doi/10.1103/PhysRevB.58.12749>
- [63] Han Q, Dang H T and Millis A J 2016 *Physical Review B* **93** ISSN 2469-9950, 2469-9969 URL <https://link.aps.org/doi/10.1103/PhysRevB.93.155103>
- [64] Hausoel A, Karolak M, Şaşıoğlu E, Lichtenstein A, Held K, Katanin A, Toschi A and Sangiovanni G 2017 *Nature Communications* **8** 16062 ISSN 2041-1723 URL <http://www.nature.com/doi/10.1038/ncomms16062>
- [65] Nguyen L, Komsa H P, Khestanova E, Kashtiban R J, Peters J J P, Lawlor S, Sanchez A M, Sloan J, Gorbachev R V, Grigorieva I V, Krasheninnikov A V and Haigh S J 2017 *ACS Nano* **11** 2894–2904 ISSN 1936-0851, 1936-086X URL <http://pubs.acs.org/doi/10.1021/acsnano.6b08036>
- [66] Jang S W, Jeong M Y, Yoon H, Ryee S and Han M J 2019 *arXiv:1904.04510 [cond-mat]* (Preprint 1904.04510) URL <http://arxiv.org/abs/1904.04510>
- [67] McQueen T M, Huang Q, Ksenofontov V, Felser C, Xu Q, Zandbergen H, Hor Y S, Allred J, Williams A J, Qu D, Checkelsky J, Ong N P and Cava R J 2009 *Phys. Rev. B* **79** 014522 URL <https://link.aps.org/doi/10.1103/PhysRevB.79.014522>
- [68] Li S, de la Cruz C, Huang Q, Chen Y, Lynn J W, Hu J, Huang Y L, Hsu F C, Yeh K W, Wu M K and Dai P 2009 *Physical Review B* **79** ISSN 1098-0121, 1550-235X URL <https://link.aps.org/doi/10.1103/PhysRevB.79.054503>
- [69] Han M J and Savrasov S Y 2009 *Phys. Rev. Lett.* **103** 067001 URL <https://link.aps.org/doi/10.1103/PhysRevLett.103.067001>
- [70] Verchenko V Y, Tsirlin A A, Sobolev A V, Presniakov I A and Shevelkov A V 2015 *Inorganic Chemistry* **54** 8598–8607 ISSN 0020-1669, 1520-510X URL <http://pubs.acs.org/doi/10.1021/acs.inorgchem.5b01260>
- [71] May A F, Calder S, Cantoni C, Cao H and McGuire M A 2016 *Physical Review B* **93** ISSN 2469-9950, 2469-9969 URL <https://link.aps.org/doi/10.1103/PhysRevB.93.014411>
- [72] Liu Y, Ivanovski V N and Petrovic C 2017 *Physical Review B* **96** ISSN 2469-9950, 2469-9969 URL <https://link.aps.org/doi/10.1103/PhysRevB.96.144429>

- [73] Liu Y, Stavitski E, Attenkofer K and Petrovic C 2018 *Physical Review B* **97** ISSN 2469-9950, 2469-9969 URL <https://link.aps.org/doi/10.1103/PhysRevB.97.165415>
- [74] Akgenc B, Mogulkoc A and Durgun E 2020 *Journal of Applied Physics* **127** 084302 ISSN 0021-8979, 1089-7550 URL <http://aip.scitation.org/doi/10.1063/1.5140578>